Available online at www.sciencedirect.com
SCIENCE DIRECT®
Journal of Catalysis 227 (2004) 138–147
JOURNAL OF CATALYSIS
www.elsevier.com/locate/jcat

Benzene hydroxylation over FeZSM-5 catalysts: which Fe sites are active?

Igor Yuranov, Dmitri A. Bulushev, Albert Renken, Lioubov Kiwi-Minsker *

Laboratory of Chemical Reaction Engineering, Swiss Federal Institute of Technology, LGRC-EPFL, CH-1015 Lausanne, Switzerland

Received 5 April 2004; revised 7 June 2004; accepted 10 June 2004

Available online 5 August 2004

Abstract

FeZSM-5 with a wide range of Fe content (0.015–2.1 wt%) were studied in the benzene hydroxylation to phenol with nitrous oxide (C_6H_6:N_2O = 1:5) at low temperatures (< 550 K). Catalysts were activated before the reaction by steaming and/or calcinations in He (1323 K). High selectivity of benzene-to-phenol transformation (> 98%) was obtained within 3 h without any deactivation of the catalyst. Three types of Fe(II) sites were formed in the zeolites extraframework due to activation and are attributed to: (1) Fe(II) sites in mononuclear species, (2) oligonuclear species with at least two oxygen-bridged Fe(II) sites, and (3) Fe(II) sites within Fe_2O_3 nanoparticles. The degree of nuclearity of Fe(II) species was observed to increase with iron content and activation temperature/time. The total amount of Fe(II) sites was monitored by the transient response method of the N_2O decomposition (523 K) accompanied by the formation of surface atomic oxygen $(O)_{Fe}$. Only mono- and oligonuclear Fe(II) sites active in CO oxidation seem also to be responsible for the FeZSM-5 activity in benzene hydroxylation. Their amount was measured by the transient response of CO_2 during CO oxidation on zeolites preloaded by $(O)_{Fe}$. The turnover frequencies in the benzene oxidation were constant independently of the catalyst activation in the isomorphously substituted zeolites. The Fe(II) ions in nanoparticles (inactive in hydroxylation) are probably irreversibly reoxidized by N_2O to Fe(III), which are known to be responsible for the total oxidation of benzene.

Keywords: Fe-containing HZSM-5; α-Oxygen; Oxo-bridged Fe(II) species; One-step benzene to phenol oxidation; Nitrous oxide decomposition with surface oxygen loading; Transient response method; Temperature-programmed desorption of oxygen

1. Introduction

ZSM-5 zeolites have been reported to be efficient catalysts for the hydroxylation of benzene to phenol by nitrous oxide with selectivity to phenol close to 100% at about 50% conversion of benzene [1–4]. The catalytic performance is due to iron in the zeolites [5–9]. Different forms of iron have been identified in the FeZSM-5 zeolites [10–16]: (1) isolated ions isomorphously substituted in the MFI framework; (2) ions in cation-exchange positions; (3) iron complexes of low nuclearity in extraframework positions; (4) Fe oxide nanoparticles of < 2 nm size in the micropores; and (5) large Fe oxide particles (2–25 nm) located at the external surface of zeolite crystals. However, only a small part of the total iron is usually active in the hydroxylation of benzene [5,7,8]. Even traces of iron (200–500 ppm) in commercial zeolites are active in this reaction after steaming and/or high-temperature calcination. There is a consensus that such activation leads to the extraframework Fe(II) species stabilised via Fe–O–Al complexes in the zeolite micropores. However, the structure of the Fe(II) sites active in hydroxylation of benzene is a subject of controversy. Jia et al. [9] postulate that mononuclear Fe sites are crucial for the benzene oxidation to phenol. By contrast, Panov and co-workers. [8,17] claim that active iron exists in the form of binuclear Fe(II) complexes generated by the autoreduction of Fe(III) during catalyst activation. These binuclear Fe(II) sites seem to be stable in the presence of O_2 but can reversibly interact with N_2O at 523 K, generating so-called "α-oxygen" species.

* Corresponding author.
E-mail address: lioubov.kiwi-minsker@epfl.ch (L. Kiwi-Minsker).

0021-9517/$ – see front matter
doi:10.1016/j.jcat.2004.06.014

This α-oxygen is responsible for the benzene hydroxylation and low-temperature oxidation of CO and CH_4 [18]. Each Fe atom in the binuclear complex is capable of generating one α-oxygen atom. The binuclear structure of Fe(II) active sites has been also suggested by Hensen and co-workers [19,20]. In this case only one oxygen atom was found per two Fe(II) atoms. Low-temperature N_2O decomposition forming active surface oxygen $(O)_{Fe}$ and gaseous N_2 has been proposed for the quantitative determination of the Fe(II) sites active in hydroxylation [21]. The reaction was assumed to proceed through the stoichiometric deposition of one oxygen atom per each active Fe(II) atom. We have recently shown [22] that only a part of the deposited oxygen ($\sim 65\%$) is active in CO oxidation. Based on Mössbauer spectra and O_2 isotopic exchange measurements, some authors discriminate two different states of Fe(II) in FeZSM-5 catalysts [8,15,17, 19,20,23]. Thus, the structure and role in the catalysis by the Fe(II)-containing species are still unclear. Different species may be responsible for the catalyst activity in different reactions: during the direct N_2O decomposition oligonuclear species are preferred over isolated Fe ions in view of the easier oxygen recombination from two neighboring Fe(II) centers, while mononuclear Fe(II) sites would be more active in oxidation reactions [24].

The present study aims to find a correlation between the activity of FeZSM-5 zeolites during benzene hydroxylation and different types of Fe(II) sites in the catalyst. For this purpose, a variety of Fe-containing ZSM-5 catalysts were prepared by different methods. The Fe content in the zeolites ranged from 0.015 to 2.1 wt%. The catalysts were activated by steaming and/or high-temperature treatment in He (1323 K). The Fe sites formed in the zeolites were characterized quantitatively by the transient response method in (1) low-temperature N_2O decomposition with the formation of surface atomic oxygen, $(O)_{Fe}$ and gaseous nitrogen, (2) CO oxidation by the surface $(O)_{Fe}$ loaded from N_2O, and by (3) temperature-programmed desorption (TPD) of O_2.

2. Experimental

2.1. Catalyst preparation

Both commercial and homemade ZSM-5 zeolites were used in the present study (Table 1). The industrial Zeocat PZ-2/50H ($Si/Al = 25$, H form) extrudates ($ZSM\text{-}5_{5500}$) and powder ($ZSM\text{-}5_{150}$) were kindly provided by Zeochem AG (Uetikon, Switzerland). The binder applied during the preparation of the catalyst contains Fe and is a reason for the high iron content in $ZSM\text{-}5_{5500}$ extrudates (~ 0.55 wt% or 5500 ppm). The isomorphously substituted $ZSM\text{-}5_{350}$ ($Si/Al = 42$) and $ZSM\text{-}5_{5800}$ ($Si/Al = 25$) were prepared by hydrothermal synthesis. Typically, tetraethylorthosilicate (TEOS, Fluka, 98%) was added to an aqueous solution of tetrapropylammonium hydroxide (TPAOH, Fluka, 20% in water) used as a template, $NaAlO_2$ (Riedel-de Haën, Na_2O, 40–45%; Al_2O_3, 50–56%), and $Fe(NO_3)_3 \cdot 9H_2O$ (Fluka, 98%). The molar ratios between components were $TEOS{:}TPAOH{:}NaAlO_2{:}H_2O = 0.8{:}0.1{:}0.016\text{–}0.032{:}33$ and $Si{:}Fe = 160{:}3200$. The mixture was stirred for 3 h at room temperature, and the final transparent gel was transferred to a stainless-steel autoclave lined with Teflon and kept in an oven at 450 K for 2 days. The product was filtered, washed with deionized water, and calcined in air at 823 K for 12 h. The zeolite was then converted into the H form by an exchange with a NH_4NO_3 aqueous solution (0.5 M) and subsequent calcination at 823 K for 3 h.

Postsynthesis iron deposition on the zeolites was performed by ion exchange with $Fe(NO_3)_3 \cdot 9H_2O$ aqueous solution (0.1 M) for 1.4% $FeZSM\text{-}5_{5500}$, 0.18% $Fe/ZSM\text{-}5^{st}_{150}$, and 0.44% $FeZSM\text{-}5_{150}$ and by adsorption from a $Fe(CH_3COO)_3$ aqueous solution (0.01 M) for 2.1% $FeZSM\text{-}5_{150}$.

The catalysts were activated via both steaming (H_2O partial pressure of 0.3 bar; He flow rate, 50 $ml\,min^{-1}$) at 823 K for 4 h and by treatment at 1323 K in a He flow (50 $ml\,min^{-1}$) for 1 h. Sometimes, Fe deposition was performed after activation. The main characteristics of the catalysts used in this study are shown in Table 1.

2.2. Catalyst characterization

The chemical composition of the catalysts was determined by atomic absorption spectroscopy (AAS) via a Shimadzu AA-6650 spectrometer. The samples were dissolved in hot aqua regia containing several drops of HF.

The specific surface areas (SSA) of the catalysts were measured using N_2 adsorption–desorption at 77 K via a Sorptomatic 1990 instrument (Carlo Erba) after catalyst pretreatment in vacuum at 523 K for 2 h. The SSA of the samples was calculated employing the BET method while the Dollimore/Heal method was applied for the calculation of pore volume.

X-ray diffraction (XRD) patterns of catalysts were obtained on a Siemens D500 diffractometer with $Cu K\alpha$ monochromatic radiation ($\lambda = 1.5406$ Å).

Three methods for the determination of the Fe(II) sites in FeZSM-5 were performed with a Micromeritics AutoChem 2910 analyzer as described below:

Method 1: The concentration of the Fe(II) sites involved in the formation of surface oxygen $(O)_{Fe}$ from N_2O, $C^{N_2O}_{Fe}$, was measured via the transient response method during N_2O decomposition over the catalysts at 523 K:

$$N_2O + (\,)^{N_2O}_{Fe} = N_2 + (O)^{N_2O}_{Fe}. \quad (1)$$

The reaction gas phase was monitored in the reactor outlet after switching in the inlet from He to a mixture 2 vol% N_2O + 2 vol% Ar + 96 vol% He. Before the measurements the samples were pretreated in He at 823 K for 1 h and then cooled in He to the temperature of the transient response experiments. The gas-phase composition as a function of time for some ZSM-5 catalysts is presented in Figs. 1a and 2a.

Table 1
The main characteristics of the FeZSM-5 catalysts

Catalyst	Fe loading		Method of catalyst activation	Fe(II) sites, C_{Fe} (10^{18} site g^{-1})			R (mmol h^{-1} g^{-1}), 543 K	E_a (kJ mol^{-1}), 523–593 K
	(wt%)	C (10^{18} atom g^{-1})		N_2O	TPD	CO		
Isomorphously substituted catalysts								
1. $ZSM\text{-}5^{calc}_{150}$	0.015	1.6	1323 K, He	0.55	0.34		0.036	
$ZSM\text{-}5^{st}_{150}$	0.015	1.6	Steaming	0.5	0.05	0.28	0.007	
2. $ZSM\text{-}5^{calc}_{350}$	0.035	3.8	1323 K, He	3.0	2.0	2.06	0.072	75.3
$ZSM\text{-}5^{st\text{-}calc}_{350}$ [a]	0.035	3.8	Steaming + 1323 K, He	2.8	1.9		0.079	76.4
$ZSM\text{-}5^{st}_{350}$	0.035	3.8	Steaming	0.8	0.13	0.47	0.032	76.2
$ZSM\text{-}5^{n}_{350}$	0.035	3.8	No	0.9	–		0.002	
3. $ZSM\text{-}5^{calc}_{5800}$	0.58	62.4	1323 K, He	11.1	10.3	9.1	0.288	
$ZSM\text{-}5^{calc}_{5800}$, 11 h[b]	0.58	62.4	1323 K, He, 11 h	6.34	4.4		0.132	
$ZSM\text{-}5^{st}_{5800}$	0.58	62.4	Steaming	7.33	2.38	3.34	0.126	
Postsynthesis Fe(III) ion-exchanged catalysts								
4. $ZSM\text{-}5^{calc}_{5500}$	0.55	59.1	1323 K, He	3.4	2.6	2.6	0.072	76.6
$ZSM\text{-}5^{st\text{-}calc}_{5500}$ [a]	0.55	59.1	Steaming + 1323 K, He	3.0	1.8		0.072	
$ZSM\text{-}5^{st}_{5500}$	0.55	59.1	Steaming	0.64	0.2		0.050	
5. 2.1% $FeZSM\text{-}5^{calc}_{150}$	2.1	225.8	1323 K, He	24.3	10.1	15.1	0.202	
2.1% $FeZSM\text{-}5^{st}_{150}$	2.1	225.8	Steaming	28.9	11.6	18.6	0.216	
6. 1.4% $FeZSM\text{-}5^{calc}_{5500}$	1.4	150.5	1323 K, He	8.4	5.1		0.133	
1.4% $FeZSM\text{-}5^{st}_{5500}$	1.4	150.5	Steaming	12.7	1.3		0.076	
1.4% $FeZSM\text{-}5^{n}_{5500}$	1.4	150.5	No	3.31	0.17		0.031	
7. 0.44% $Fe/ZSM\text{-}5^{st}_{150}$	0.44	47.3	Steaming before ion exchange	12.5	1.0		0.094	
8. 0.18% $Fe/ZSM\text{-}5^{st}_{150}$	0.18	19.4	Steaming before ion exchange	2.3	0.31		0.032	

"Steaming" means activation water vapor at 823 K for 4 h; "1323 K, He" means activation in flow of He (60 ml min^{-1}) at 1323 K for 1 h.
[a] The catalysts were steamed before the 1323 K treatment in He.
[b] The catalyst was heated in He at 1323 K for 11 h.

The reaction (1) was assumed to proceed through evolution of a stoichiometric amount of N_2 into the gas phase and deposition of one oxygen atom per each Fe(II) [21]. The $C_{Fe}^{N_2O}$ was determined by integration of the peak of the released nitrogen.

Method 2: The deposited oxygen, which is able to recombine forming O_2 and concentration of the corresponding Fe(II) sites, C_{Fe}^{TPD}, were estimated from the amount of molecular oxygen evolved during temperature-programmed desorption (523–873 K). The TPD analysis was performed immediately after the sample treatment by N_2O at 523 K (deposition of $(O)_{Fe}$). The TPD oxygen profile is shown in Fig. 1b.

Method 3: The deposited oxygen, which is active in low-temperature (553 K) CO oxidation, $(O)_{Fe}^{CO}$, was measured via the transient response of CO_2 during CO oxidation at 523 K performed immediately after the sample treatment by N_2O at 523 K (deposition of $(O)_{Fe}$) according to the reaction:

$$CO + (O)_{Fe}^{CO} = CO_2 + (\,)_{Fe}^{CO}. \quad (2)$$

The concentration of the corresponding Fe(II) sites, C_{Fe}^{CO}, was determined assuming that one active oxygen atom can attach to one Fe(II) site. During the measurements the reaction gas phase was monitored in the reactor outlet after switching in the inlet from He to a mixture 3 vol% CO + 97 vol% He. The gas-phase composition as a function of time for the $ZSM\text{-}5^{calc}_{350}$ sample is presented in Fig. 2b. The C_{Fe}^{CO} was determined by integration of the peak of the released CO_2.

These methods have been described in detail elsewhere [22].

2.3. Catalyst testing

The FeZSM-5 catalysts were tested in the benzene hydroxylation with N_2O as prepared or after different activations. The catalyst activation was carried out by steaming and/or high-temperature treatment in He ($T = 1323$ K). Hydroxylation was carried out in a vertical stainless-steel fixed-bed reactor (inner diameter, 20 mm) at 510–600 K and atmospheric pressure. The catalyst ($m = 0.3$–1.0 g,

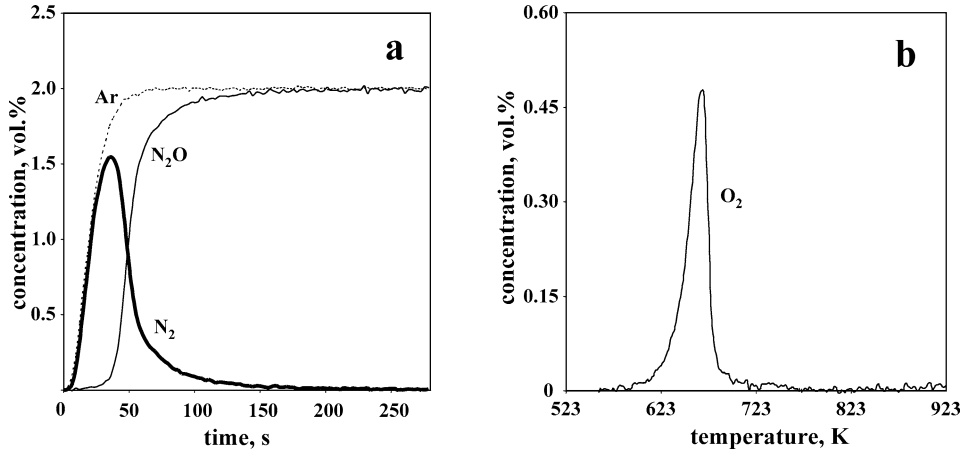

Fig. 1. (a) Transient response at 523 K obtained after the switch from He to the 2 vol% N_2O + 2 vol% Ar + 96 vol% He mixture over ZSM-5^{calc}_{5800} catalyst (pretreatment in He, 1323 K, 1 h; $m_{cat} = 0.503$ g); (b) temperature-programmed desorption of oxygen from ZSM-5^{calc}_{5800} catalyst after the surface oxygen loading from N_2O.

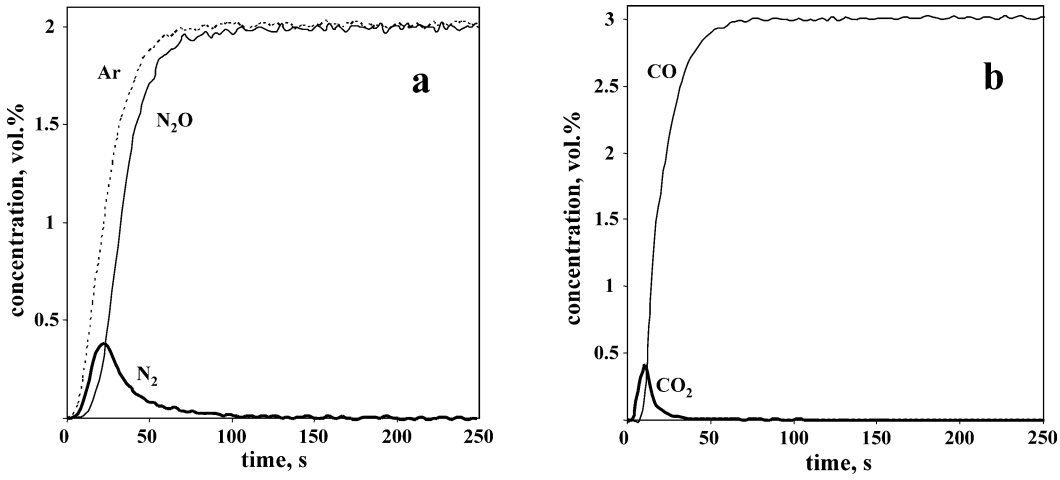

Fig. 2. (a) Transient response at 523 K obtained after the switch from He to the 2 vol% N_2O + 2 vol% Ar + 96 vol% He mixture over ZSM-5^{st}_{350} catalyst (pretreatment in He, 823 K, 1 h; $m_{cat} = 0.949$ g); (b) transient response at 523 K obtained after the switch from He to the 3 vol% CO in He over ZSM-5^{st}_{350} catalyst after the surface oxygen loading from N_2O.

$d_p = 0.2$–0.5 mm) was placed on a plate of sintered stainless-steel fibers, which was fixed in the middle of the reactor. The catalyst was mixed with inert silica grains to form a uniform catalyst bed of 3–4 mm height. The mixture of 1 vol% of benzene, 5 vol% of N_2O, and 94 vol% of He was used for the catalytic tests. Before reaction, the catalyst was pretreated in He at 773 K for 2 h to remove moisture and other volatile contaminations. The gases were provided by Carbagas (Lausanne, Switzerland, > 99.99%) and used as received. Benzene was fed into the reactor by passing He through a thermostated ($T = 293$ K) bubble column. The gas flow was controlled by mass-flow controllers. The total gas flow of 60 ml(STP) min^{-1} was used throughout the study. The reaction temperature was monitored by a thermocouple placed in the catalytic bed. The reaction mixture was analyzed on-line by GC (Perkin-Elmer Autosystem XL). The organic components were separated in a SPB-5 capillary column and detected by FID. The light gases (N_2, N_2O, CO, CO_2) were separated in a Carboxen-1010 capillary column and detected by TCD.

3. Results and discussion

3.1. Catalysts

Various Fe-containing ZSM-5 catalysts having different iron loading were used in order to elucidate the Fe sites catalyzing the phenol hydroxylation with N_2O (Table 1). The industrial zeolite ZSM-5_{150} (powder) was found to contain only traces of iron (∼ 150 ppm). But the same industrial zeolite ZSM-5_{5500} (extrudates) contained ∼ 5500 ppm of Fe. This difference is due to the binder containing Fe applied during the extrusion step of the zeolite production. Clearly, iron in the ZSM-5_{5500} is mostly in the form of big Fe oxide particles on the surface of zeolite crystallites. To introduce

Fe ions directly in cation-exchange extraframework positions in the channels of the industrial parent zeolites, ion exchange or adsorption from the aqueous solutions of Fe(III) nitrate or Fe(III) acetate were performed (samples 5–8 in Table 1). The final Fe loadings (wt%) were varied by changing the concentration of the Fe solutions and are indicated in the catalyst designations.

The ZSM-5_{350} and ZSM-5_{5800} zeolites were prepared by the hydrothermal synthesis. In order to obtain a low (350 ppm) and high (5800 ppm) content of isomorphously substituted iron in the zeolite, the Fe(III) nitrate was added into the initial silica gel. The synthesized samples exhibited an X-ray diffraction pattern typical for the MFI framework. No formation of a bulk Fe oxide phase was observed.

The catalysts were activated by either steaming or high-temperature treatment in He ($T = 1323$ K) as indicated in the catalyst designations. The beneficial effect of the steaming pretreatment on the activity of ZSM-5 catalysts during the benzene hydroxylation with N_2O is well known [6,9,19]. Steam treatment leads to significant dealumination of zeolite lattice and expulsion of isomorphously substituted Fe(III). This process is accompanied by partial Fe(III) autoreduction and the formation of extraframework Fe(II)–O–Al species [15,20]. The high-temperature treatment in He is suggested to drastically increase of the concentration of Fe(II) sites, which are capable of forming surface atomic oxygen $(O)_{Fe}$ from N_2O [22].

In the case of the 0.18% Fe/ZSM-5^{st}_{150} and 0.44% Fe/ZSM-5^{st}_{150} catalysts, Fe deposition by ion exchange was performed after steaming of the parent zeolite. Steam treatment of zeolites is known to lead to a decrease in the concentration of Brønsted sites [6,15] resulting in the reduction of the ion-exchange capacity.

3.2. Determination of active Fe(II) sites

3.2.1. Fe(II) sites involved in surface oxygen loading from N_2O (Method 1)

Zeolite titration at low temperature and pressure by N_2O forming atomic surface oxygen $(O)_{Fe}$ and gaseous N_2 was used for the quantitative determination of the Fe(II) sites active in oxidation and hydroxylation [21]. Recently, we proposed the transient response in N_2O decomposition over zeolites for the same purpose [22]. The method is used in the present study, and the results are presented in Figs. 1a and 2a as the concentration–time profiles in the reactor outlet after switching from He to N_2O. The nonideal reactor behavior (as compared to a plug-flow reactor) is characterized by inert tracer argon (Ar). As seen, N_2 appears in the outlet simultaneously with Ar, and a delay is observed for N_2O appearance. No O_2 was detected in the outlet, indicating that only reaction (1) takes place. The concentration of Fe(II) sites participating in the formation of surface oxygen $(O)_{Fe}$ via N_2O decomposition, $C_{Fe}^{N_2O}$, was calculated from the amount of N_2 released. A single oxygen atom was assumed to chemisorb on each Fe(II) site [21]. Depending on the iron content in the zeolites and their activation applied, the $C_{Fe}^{N_2O}$ varied over two orders of magnitude from $\sim 5 \times 10^{17}$ to 3×10^{19} sites g^{-1} (Table 1).

The $C_{Fe}^{N_2O}$ in general increases with the Fe loading. A higher Fe loading means a higher amount of the Fe(II) sites able to accept atomic oxygen from N_2O. This is observed for isomorphously substituted and postsynthesis modified zeolites (catalysts 3 and 5 in Table 1). However, no direct relationship between the $C_{Fe}^{N_2O}$ and the total Fe content in zeolites reported in [7,25] was found. The number of the sites, $C_{Fe}^{N_2O}$, correlates with the amount of Fe(II) generated during the zeolite activation [15,20]. The formation of Fe(II) sites was observed during calcination of zeolites in air at 823 K (synthesis) and for zeolites pretreated at 823 K in He before the measurements (see the nonactivated ZSM-5^{n}_{350} and 1.4% Fe/ZSM-5^{n}_{5500} in Table 1). The final concentration of the Fe(II) sites, $C_{Fe}^{N_2O}$, depends on the method of Fe introduction into the zeolite and its activation. The number of the formed Fe(II) sites is considerably lower for the postsynthesis modified zeolites. About 25% of Fe atoms in the 0.44% Fe/ZSM-5^{st}_{150}, which was steamed before the ion exchange with Fe, were found active toward the formation of surface atomic oxygen. At the same time, $\sim 80\%$ of the total amount of iron atoms in the isomorphously substituted ZSM-5^{calc}_{350} after high-temperature activation in He were able to form $(O)_{Fe}$. The latter result indicates that each Fe atom in the active complexes in zeolites with a low Fe content can decompose N_2O attaching an oxygen atom. This result is in line with the reports [8,9], but it is in variance with the study [20] claiming that about one oxygen atom is formed per two Fe(II) atoms.

High-temperature activation in He ($T = 1323$ K) if compared to the activation by steaming is more effective for conversion of isomorphously substituted Fe(III) ions to Fe(II) sites. The concentration of Fe(II) sites ($C_{Fe}^{N_2O}$) in the catalysts 2–4 after this treatment was found to be 3–4 times higher than after steaming (Table 1). The reverse situation is observed for the postsynthesis modified zeolites with a high Fe loading (catalysts 5 and 6). In this case, after Fe(III) cation exchange followed by steaming of the zeolites, the attained $C_{Fe}^{N_2O}$ was extremely high ($1.3–2.9 \times 10^{19}$ sites g^{-1}). Since these zeolites contain quite large amounts of iron (1.4–2.1 wt%), the formation of Fe(III) oxide particles in the zeolite pores after the high-temperature treatment is possible [26]. Therefore, Fe(II) sites active in N_2O decomposition are likely to be partially formed within the bulk Fe(III)-oxide nanoparticles. Indeed, two types of Fe(II) species, which react with N_2O, have been distinguished for the FeZSM-5 catalysts [15,19,20,22]. One type of the Fe(II) species generates oxygen active in CO oxidation and is capable of participating in the catalytic cycle of N_2O decomposition forming O_2 and N_2. The other Fe(II) species assigned to aggregated iron oxide is irreversibly oxidized by N_2O [19,20].

3.2.2. Determination of Fe(II) sites by temperature-programmed desorption of oxygen (Method 2)

The FeZSM-5 samples treated by N_2O at 523 K reaction (1) were immediately analyzed by TPD. The evolution of O_2 from the catalysts appeared as a sharp peak with a maximum at ∼ 670 K (Fig. 1b). Coupling of $(O)_{Fe}$ attached to the neighboring Fe atoms in the oligonuclear species containing at least two oxo-bridged Fe(II) sites [8,17,22] seems to be an easier process as compared to the recombination of distant single $(O)_{Fe}$ atoms attached to the mononuclear Fe(II) sites, which involves surface diffusion. In this case, the TPD of O_2 would appear as a broad peak [22] with a maximum at higher temperatures. Thus, we propose that the oligonuclear oxo-bridged Fe(II) species are responsible for the sharp O_2 peak observed at ∼ 670 K in TPD from the samples treated in N_2O at low temperatures. Since we have no direct proof for the species structure, we suggest for the sake of simplicity to present Fe(II) sites in oligonuclear species as binuclear Fe(II) sites. Therefore, from now on the oligonuclear Fe(II) site is named as a binuclear one.

The concentrations of the binuclear Fe(II) active sites, C_{Fe}^{TPD}, are presented in Table 1. The C_{Fe}^{TPD} was found to vary over a wide range (1×10^{17}–1×10^{19} sites g^{-1}), but never attained the $C_{Fe}^{N_2O}$ ($C_{Fe}^{TPD} < C_{Fe}^{N_2O}$). The binuclear Fe(II) active sites formation was found to depend on the method of catalyst activation (Table 1). A fraction of the binuclear Fe(II) sites in the steamed catalysts was only ∼ 10–40% of the $C_{Fe}^{N_2O}$, while after the high-temperature calcinations in He it increased up to 40–90%. This difference is especially pronounced for the isomorphously substituted zeolites with a low Fe loading. The C_{Fe}^{TPD} was ∼ 4% of the total Fe loading in the nontreated ZSM-5_{350}^{st}, but increased up to 55% after the high-temperature activation (ZSM-5_{350}^{calc}). Steaming of the catalyst before the high-temperature activation (see the ZSM-$5_{350}^{st\text{-}calc}$ in Table 1) did not change the final C_{Fe}^{TPD}. Thus, we conclude that the zeolite activation in He at 1323 K is an effective method for the formation of the binuclear Fe(II) active sites.

3.2.3. Fe(II) sites active in CO oxidation (Method 3)

It has been recently reported [22] that in the isomorphously substituted zeolites activated in He at 1323 K the concentration of oxygen deposited on binuclear Fe(II) active sites, which evolves as a sharp peak at ∼ 670 K during TPD (C_{Fe}^{TPD}), is close to the amount of oxygen active in CO oxidation at 523 K (C_{Fe}^{CO}). This observation was confirmed in the present study for the zeolites after high-temperature activation (see the ZSM-5_{350}^{calc}, ZSM-5_{5500}^{calc}, ZSM-5_{5800}^{calc} in Table 1). However, it was found that in the steamed catalysts the concentration of oxygen active in CO oxidation is considerably higher than the C_{Fe}^{TPD}. This result indicates that some sites additional to the binuclear ones exist in the steamed FeZSM-5 catalysts. These sites also generate the surface $(O)_{Fe}$ active in low-temperature CO oxidation, but this oxygen does not appear in TPD below 873 K. The mononuclear structure of the Fe(II) sites seems to account for such behavior. Indeed, unlike the easy coupling of $(O)_{Fe}$ in binuclear Fe(II) centers, recombination of oxygen atoms attached to the mononuclear Fe sites involves surface diffusion. Therefore, the O_2 evolution would appear in the TPD profile as a broad peak at temperatures much higher than 670 K, unless the diffusing oxygen atoms interact with various Fe species present at higher iron concentrations. Mononuclear Fe(II) active sites are mostly detected in the isomorphosly substituted FeZSM-5 zeolites steamed at 823 K. After the high-temperature activation in He the formation of binuclear Fe(II) active sites is favored. At the same time, the formation of iron oxide nanoclusters in the zeolite micropores and the formation of big particles on the outer surface of crystallites were observed [15].

3.3. Catalyst activity in benzene hydroxylation

One-step oxidation of benzene to phenol was carried out in the reaction mixture of 1 vol% C_6H_6 + 5 vol% N_2O + 94 vol% He. The reaction temperature range of 510–590 K was chosen in order to avoid catalytic decomposition of N_2O with the formation of O_2 and N_2. This process takes place at temperatures higher than 570–580 K [22] leading to low selectivity of N_2O toward phenol formation. The time dependence of benzene conversion over the ZSM-5_{5500} catalyst is presented in Fig. 3. The catalyst performance is stable at temperatures as high as 543 K within 3 h. At the same time, the selectivity of benzene transformation to phenol was > 98%. At higher temperatures, catalyst deactivation is observed with a small loss of selectivity toward phenol (95–98%).

It is well known that benzene hydroxylation with N_2O over zeolites at temperatures 620–720 K is accompanied by a pronounced catalyst deactivation due to coke formation in the zeolite micropores [6,14,27–31]. A high initial activity is followed by a strong deactivation reaching a steady state after 2–3 h. Molecular oxygen produced at elevated temperatures due to N_2O decomposition participates in the coke formation (polycondensation of phenols) leading to site poisoning. To avoid this, all measurements of catalytic activity

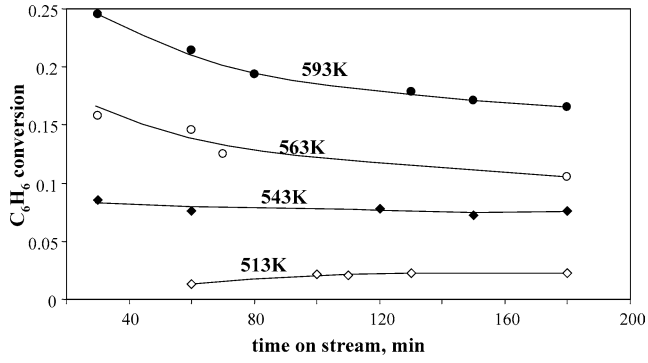

Fig. 3. Benzene to phenol oxidation over ZSM-5_{5500}^{calc} catalyst at different temperatures: m_{cat} = 1.0 g; C_6H_6:N_2O = 1:5; total gas flow = 60 ml min^{-1}.

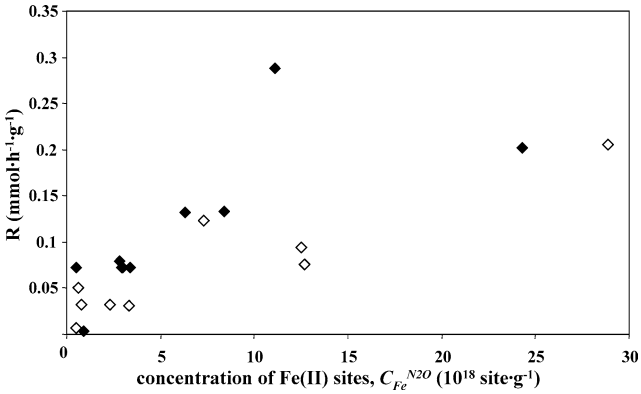

Fig. 4. The rate of benzene to phenol oxidation as a function of Fe(II) sites concentration determined via titration by N_2O ($C_{Fe}^{N_2O}$) of different FeZSM-5 catalysts activated by: (◆) steaming at 823 K; (◇) calcinations in He at 1323 K for 1 h; C_6H_6:N_2O = 1:5; total gas flow = 60 ml min^{-1}; T = 543 K.

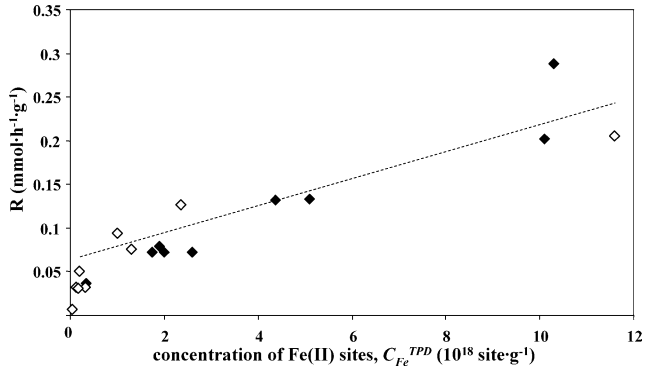

Fig. 5. The rate of benzene to phenol oxidation as a function of binuclear Fe(II) site concentrations determined via TPD of oxygen (C_{Fe}^{TPD}) of different FeZSM-5 catalysts activated by: (◆) steaming at 823 K; (◇) calcination in He at 1323 K for 1 h; C_6H_6:N_2O = 1:5; total gas flow = 60 ml min^{-1}; T = 543 K.

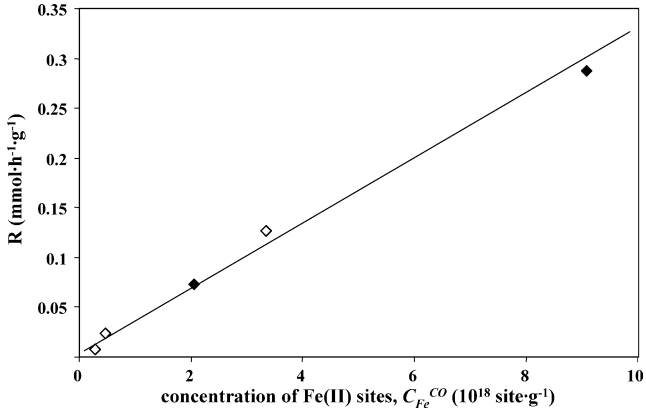

Fig. 6. The rate of benzene to phenol oxidation as a function of the concentration of Fe(II) sites active in CO oxidation (C_{Fe}^{CO}) determined in the isomorphously substituted FeZSM-5 catalysts activated by: (◆) steaming at 823 K; (◇) calcination in He at 1323 K for 1 h; C_6H_6:N_2O = 1:5; total gas flow = 60 ml min^{-1}; T = 543 K.

were performed at 543 K after 2 h on steam. The obtained phenol productivities R are collected in Table 1. The highest rates were measured for the isomorphously substituted ZSM-5^{calc}_{5800}: ∼ 0.29 mmol h^{-1} g^{-1}. For the postsynthesis Fe-modified zeolite, 2.1% FeZSM-5^{st}_{150}, the productivity to phenol of only ∼ 0.22 mmol h^{-1} g^{-1} was reached, despite the almost 4-fold higher total Fe content as compared to the isomorphously substituted sample.

In general no proportionality between R and the total Fe loading was observed for both isomorphously substituted and ion-exchanged samples independently of the activation method (steaming or/and high-temperature He calcinations). Indeed, Fe(III) oxide is known to be inactive in benzene hydroxylation. Only the Fe(II) sites, which are able to generate $(O)_{Fe}$, seem be involved in catalytic cycle. We have, therefore, plotted (Fig. 4) the reaction rate, R, as a function of the total amount of the Fe(II) sites, $C_{Fe}^{N_2O}$. It is clearly seen that no relationship exists between the rate of phenol formation and the amount of Fe(II) adsorbing atomic oxygen at low temperatures from N_2O. This result indicates that not all $(O)_{Fe}$ loaded from N_2O is active in the phenol formation, lending distrust to the definition of α-oxygen [21].

Based on the statement by Panov and co-workers [21] that α-oxygen active in oxidation is formed by binuclear Fe(II) sites, we plotted R against the amount of binuclear Fe(II) sites, C_{Fe}^{TPD} (Fig. 5). A direct proportionality is seen in the region of C_{Fe}^{TPD} >1–2 × 10^{18} sites g^{-1}. The result indicates that these Fe(II) sites are responsible for the activity in benzene hydroxylation:

$$N_2O + \text{bi-}(\,)_{Fe} = N_2 + \text{bi-}(O)_{Fe}, \quad (3)$$

$$C_6H_6 + \text{bi-}(O)_{Fe} = C_6H_5OH + \text{bi-}(\,)_{Fe}. \quad (4)$$

However, at very low concentrations of the Fe(II) sites the observed proportionality decays. The mononuclear centers, which do not appear in TPD, seem to contribute substantially in benzene hydroxylation and should be also taken into consideration:

$$N_2O + \text{mono-}(\,)_{Fe} = N_2 + \text{mono-}(O)_{Fe}, \quad (5)$$

$$C_6H_6 + \text{mono-}(O)_{Fe} = C_6H_5OH + \text{mono-}(\,)_{Fe}. \quad (6)$$

Fig. 6 represents reaction rate R over the isomorphously substituted FeZSM-5 zeolites as a function of the concentration of the Fe(II) sites (mono- and binuclear) active in CO oxidation, C_{Fe}^{CO}. It follows that R is directly proportional to the total concentration of mono- and binuclear Fe(II) sites up to the C_{Fe}^{CO} ∼ 10^{19} site g^{-1}, suggesting these sites as responsible also for the activity in benzene hydroxylation. This result together with the close values for the apparent activation energies E_a found for the catalysts with different Fe contents (Table 1) points to a similar catalytic behavior of mono- and binuclear Fe(II) active sites in benzene hydroxylation.

Fig. 7 shows the reaction TOFs calculated as the rate of phenol formation referred to as C_{Fe}^{TPD} and C_{Fe}^{CO} (inset) for the catalysts studied. As seen, the TOF calculated for sum

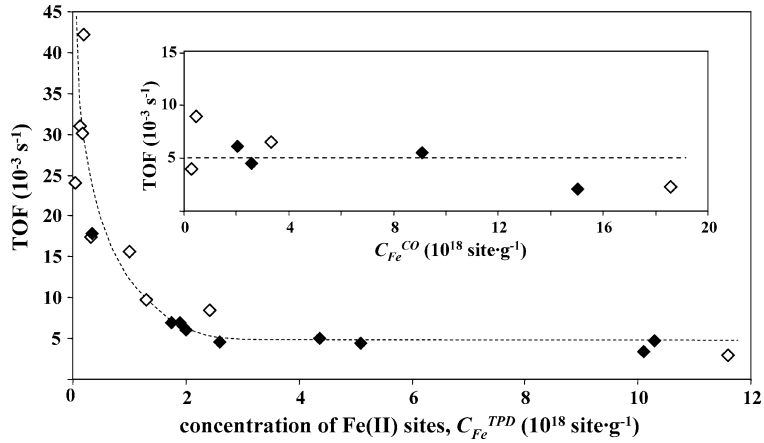

Fig. 7. Turnover frequencies (TOFs) of benzene to phenol oxidation calculated for the binuclear Fe(II) sites ($C_{\mathrm{Fe}}^{\mathrm{TPD}}$) and for the Fe(II) sites active in CO oxidation ($C_{\mathrm{Fe}}^{\mathrm{CO}}$) (inset) over different FeZSM-5 activated by: (◆) steaming at 823 K; (◇) calcination in He at 1323 K for 1 h. C_6H_6:N_2O = 1:5; total gas flow = 60 ml min^{-1}; T = 543 K.

of mono- and binuclear Fe(II) sites ($C_{\mathrm{Fe}}^{\mathrm{CO}}$) is a constant for the site concentrations less than $\sim 10^{19}$ site g^{-1}. At higher values of $C_{\mathrm{Fe}}^{\mathrm{CO}}$ obtained in the postsynthesis ion-exchanged catalysts with Fe loading of 2.1 wt%, the TOF was lower. This result can be explained by the strong influence of a big amount of Fe(III)-oxide particles formed in the zeolites, on the Fe(II) active sites measurements (determination of $C_{\mathrm{Fe}}^{\mathrm{CO}}$).

We conclude that the quantitative determination of Fe(II) active sites by the transient response of CO_2 during CO oxidation by the surface atomic oxygen $(O)_{Fe}$ is applicable only for the isomorphously substituted FeZSM-5 catalysts with a relatively low content of iron (< 0.5–0.6 wt%).

The present study shows that the activated FeZSM-5 zeolites contain different Fe(II) extraframework species. The relative content of the species depends on the total iron concentration in the zeolite, the preparation method, and activation procedure. The nuclearity of the Fe(II) species (mono-, bi-, oligonuclear species or nanoparticles) in isomorphously substituted FeZSM-5 zeolites has a tendency to increase with the total iron concentration and temperature/time of activation. This is schematically presented in Fig. 8. At very low Fe concentrations (< 350–500 ppm) and after steaming at 823 K active sites seem to exist as mononuclear extraframework Fe(II)–O–Al complexes together with some amount of centers with higher nuclearity. A high-temperature activation in He of the low Fe content zeolites creates mostly oligonuclear species containing at least two oxo-bridged Fe(II) sites. The increase of these species concentration is also observed with the increase in Fe content (> 500 ppm). At the same time, Fe(III) oxide nanoclusters begin to appear in zeolite micropores. The Fe(III) oxide nanoclusters are probably partially reduced to Fe(II) during the catalyst activation. Further increase of the Fe concentration by postsynthesis loading (ion exchange) leads to the formation of inactive agglomerates of iron (III) oxide on the external surface of the zeolite, which is responsible for the total oxidation.

The Fe(II) sites relating to mono- and oligonuclear (bi-) species and Fe(II) in iron oxide nanoparticles seem to participate in surface oxygen $(O)_{Fe}$ loading from N_2O. They can be quantitatively determined by the transient response method during low-temperature N_2O decomposition. Not all deposited atomic oxygen was found to be active for oxidation. Only the sites of low nuclearity have $(O)_{Fe}$ participating in catalytic cycles, as determined by the transient response of CO_2 during CO oxidation. The same sites seem to be responsible for the FeZSM-5 catalyst activity in the benzene hydroxylation with N_2O. Due to the easy direct recombination of the neighboring oxygen atoms, oligonuclear Fe(II) sites, unlike mononuclear ones, give a sharp peak in the TPD profile at $\sim$ 670 K. Therefore it is possible to suggest the TPD of O_2 as a quantitative method for the determination of Fe(II) sites in oligonuclear species.

4. Conclusions

1. Benzene was shown to be hydroxylated to phenol by N_2O at 550 K with high selectivity (> 98%) without catalyst deactivation within 3 h provided that Fe-ZSM5 is properly synthesized and activated. For the same Fe content and activation (steaming and/or high-temperature treatment in He), isomorphously substituted FeZSM-5 showed a higher activity as compared to the Fe ion-exchanged samples.
2. Three types of Fe(II) active sites were observed in the zeolites upon activation. They could be assigned to: (1) Fe(II) sites in mononuclear species, (2) oligonuclear species with at least two oxygen-bridged Fe(II) sites, and (3) Fe(II) sites within Fe_2O_3 nanoparticles. The total amount of Fe(II) sites was determined by the transient response method during low-temperature (523 K) N_2O decomposition accompanied by the formation of surface atomic oxygen $(O)_{Fe}$. Only mono- and oligonuclear Fe(II) sites can form $(O)_{Fe}$ active in benzene hydroxyla-

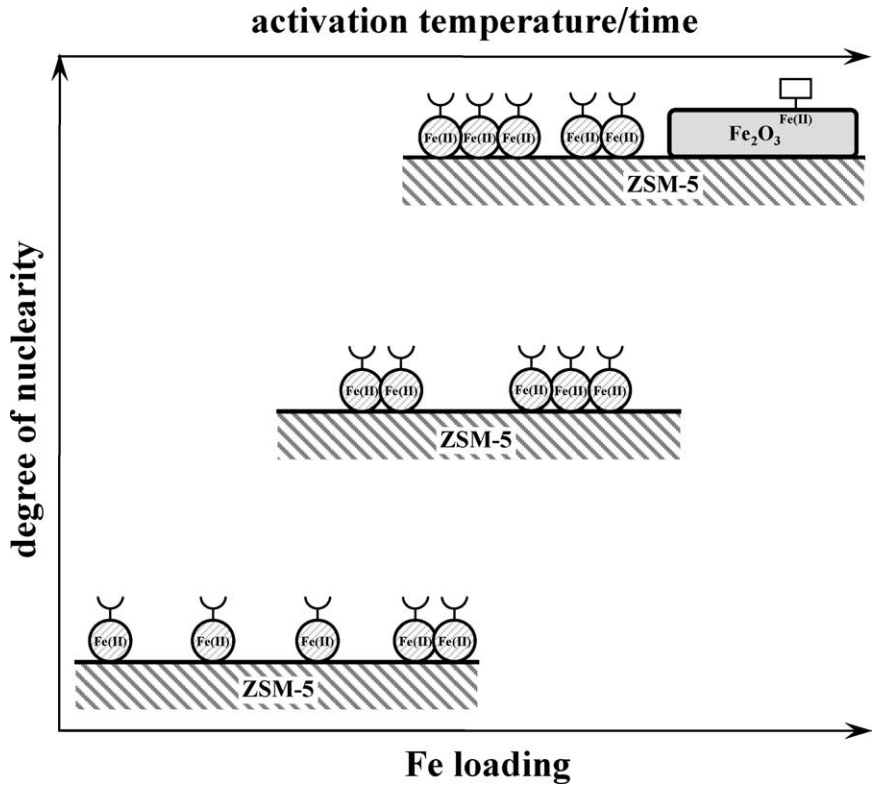

Fig. 8. Schematic presentation of the evolution of Fe(II) sites in FeZSM-5 upon activation and increase in Fe content.

tion and CO oxidation. Their amount in isomorphously substituted catalysts was measured by the transient response of CO_2 during CO oxidation (523 K) over the zeolite preloaded by $(O)_{Fe}$. The concentration of oligonuclear Fe(II) sites was determined by TPD of O_2.

3. The nuclearity of the Fe(II) species in the isomorphously substituted FeZSM-5 zeolites is a function of the iron concentration and activation method. Mononuclear Fe(II) active sites were preferably formed in the catalysts with low Fe concentrations (<350–5500 ppm) after steaming (823 K). They were transformed to the oligonuclear Fe(II) active species upon high-temperature treatment in He.
4. Mono- and oligonuclear Fe(II) sites active in CO oxidation seem also to be responsible for the FeZSM-5 activity in benzene hydroxylation. The reaction turnover frequency over isomorphously substituted zeolites (calculated as the rate of phenol formation referred to the amount of the Fe(II) sites active in CO oxidation) was observed to be constant and independent of the catalyst activation procedure (steaming and/or calcination temperature).

Acknowledgments

The authors thank A. Udriot for the chemical analysis of the samples. Financial support from the Swiss National Science Foundation is highly appreciated.

References

[1] A.S. Kharitonov, G.A. Sheveleva, G.I. Panov, V.I. Sobolev, Y.A. Paukshtis, V.N. Romannikov, Appl. Catal. A 98 (1993) 33.
[2] V.I. Sobolev, K.A. Dubkov, E.A. Paukshtis, L.V. Pirutko, M.A. Rodkin, A.S. Kharitonov, G.I. Panov, Appl. Catal. A 141 (1996) 185.
[3] G.I. Panov, Cat. Tech. 4 (2000) 18.
[4] L.M. Kustov, A.L. Tarasov, V.I. Bogdan, A.A. Tyrlov, J.W. Fulmer, Catal. Today 61 (2000) 123.
[5] P.P. Notté, Top. Catal. 13 (2000) 387.
[6] P. Kubánek, B. Wichterlová, Z. Sobalík, J. Catal. 211 (2002) 109.
[7] L.V. Pirutko, V.S. Chernyavsky, A.K. Uriarte, G.I. Panov, Appl. Catal. A 227 (2002) 143.
[8] K.A. Dubkov, N.S. Ovanesyan, A.A. Shteinman, E.V. Starokon, G.I. Panov, J. Catal. 207 (2002) 341.
[9] J. Jia, K.S. Pillai, W.M.H. Sachtler, J. Catal. 221 (2004) 119.
[10] E.M. El-Malki, R.A. van Santen, W.M.H. Sachtler, J. Phys. Chem. B 103 (1999) 4611.
[11] E.M. El-Malki, R.A. van Santen, W.M.H. Sachtler, J. Catal. 196 (2000) 212.
[12] P. Marturano, L. Drozdová, A. Kogelbauer, R. Prins, J. Catal. 192 (2000) 236.
[13] R.Q. Long, R.T. Yang, J. Catal. 194 (2000) 80.
[14] A. Ribera, I.W.C.E. Arends, S. de Vries, J. Péres-Ramíres, R.A. Sheldon, J. Catal. 195 (2000) 287.
[15] J. Pérez-Ramírez, G. Mul, F. Kapteijn, J.A. Moulijn, A.R. Overweg, A. Doménech, A. Ribera, I.W.C.E. Arends, J. Catal. 207 (2002) 113.
[16] H.Y. Chen, E.M. El-Malki, X. Wang, R.A. van Santen, W.M.H. Sachtler, J. Mol. Catal. A: Chem. 162 (2000) 159.
[17] E.V. Starokon, K.A. Dubkov, L.V. Pirutko, G.I. Panov, Top. Catal. 23 (2003) 137.
[18] G.I. Panov, A.K. Uriarte, M.A. Rodkin, V.I. Sobolev, Catal. Today 41 (1998) 365.
[19] Q. Zhu, R.M. van Teeffelen, R.A. van Santen, E.J.M. Hensen, J. Catal. 221 (2004) 575.

[20] E.J.M. Hensen, Q. Zhu, M.M.R.M. Hendrix, A.R. Overweg, P.J. Kooyman, M.V. Sychev, R.A. van Santen, J. Catal. 221 (2004) 560.
[21] G.I. Panov, V.A. Sobolev, A.S. Kharitonov, J. Mol. Catal. 61 (1990) 85.
[22] L. Kiwi-Minsker, D.A. Bulushev, A. Renken, J. Catal. 219 (2003) 273.
[23] J. Jia, B. Wen, W.M.H. Sachtler, J. Catal. 210 (2002) 453.
[24] J. Péres-Ramírez, F. Kapteijn, A. Brückner, J. Catal. 218 (2003) 234.
[25] L.V. Pirutko, A.K. Uriarte, V.S. Chernyavsky, A.S. Kharitonov, G.I. Panov, Micropor. Mesopor. Mater. 48 (2001) 345.
[26] L.J. Lobree, I.-C. Hwang, J.A. Reimer, A.T. Bell, J. Catal. 186 (1999) 242.
[27] G.I. Panov, A.S. Kharitonov, V.I. Sobolev, Appl. Catal. A 98 (1993) 1.
[28] M. Hafele, A. Reitzmann, D. Roppelt, G. Emig, Appl. Catal. A 136 (1997) 153.
[29] D.P. Ivanov, V.I. Sobolev, G.I. Panov, Appl. Catal. A 241 (2003) 113.
[30] E.J.M. Hensen, Q. Zhu, R.A. van Santen, J. Catal. 220 (2003) 260.
[31] S. Perathoner, F. Pino, G. Centi, G. Giordano, A. Kattovic, J.B. Nagy, Top. Catal. 23 (2003) 125.